Received: 26 September 2021 | Revised: 22 January 2022 | Accepted: 22 January 2022

DOI: 10.1002/pls2.10068

RESEARCH ARTICLE

SPE POLYMERS WILEY

PP-GF-EPP sandwich structures as housing materials for rechargeable energy storage system of electric vehicles: Investigations into flame retardancy

Carl-Christoph Höhne[1] | **Volker Gettwert**[1] | **Sascha Kilian**[1] | **Benjamin Tillner**[2] | **Ivonne Jahn**[2] | **Andreas Menrath**[1]

[1]Environmental Engineering, Fraunhofer Institute for Chemical Technology ICT, Pfinztal, Germany

[2]Thermoplastic Fiber Composite Semi-Finished Products, Fraunhofer Institute for Microstructure of Materials and Systems IMWS, Schkopau, Germany

Correspondence
Carl-Christoph Höhne, Environmental Engineering, Fraunhofer Institute for Chemical Technology ICT, Joseph-von-Fraunhofer Str. 7, Pfinztal 76327, Germany.
Email: carl-christoph.hoehne@ict.fraunhofer.de

Abstract

The growing importance of electric mobility has led to an increased demand for safety technologies in the automotive sector, such as the flame retardancy of materials used for electric vehicles. The fire protection of a fully equipped rechargeable energy storage system (REESS), including battery, housing, control electronics, etc., against a fuel fire must be tested according to UNECE Regulation No. 100 Annex 8E - Fire Resistance (UNECE-R100-8E). To pass this fire retardancy requirement, the flame retardancy of the housing materials is of great importance. In this study, the flame retardancy of glass-fiber-reinforced polypropylene (PP-GF) tape laminates containing the flame retardant magnesium hydroxide and different GF amounts, as well as sandwich structures of these PP-GF tape laminates with a polypropylene bead foam (EPP) core, are investigated by a limiting oxygen index test, a UL94 test and a cone calorimeter test. Furthermore, a newly developed approach of a bench-scale fuel fire test which simulates the fire treatment of the UNECE-R100-8E on component level is used.

KEYWORDS

bead foam, bench-scale fuel fire test, cone calorimeter, electric mobility, flame retardant, glass-fiber-reinforced tapes, limiting oxygen index, magnesium hydroxide, polypropylene, rechargeable energy storage system, sandwich, UL94

1 | INTRODUCTION

The growing importance of electric mobility is causing many changes within the automotive sector. One such change is the increased demand for safety technologies, especially for the rechargeable energy storage system (REESS). Battery cells, which store the energy in a REESS, are sensitive to thermal treatment. Even if just one battery cell is damaged, a thermal runaway of the whole battery module or even the entire battery pack may occur.[1] Beside the propagation of a long and hot burning fire, explosions and the release of toxic fluorine-containing gases and carcinogenic heavy metal particles are a major risk. The temperature inside a REESS is therefore well controlled. To protect the battery cells of a REESS in a post-car-accident fire, possibly caused by a burning pool of car fluids, the REESS must fulfill strict fire retardancy requirements. According to UNECE Regulation No. 100 Annex 8E - Fire Resistance,[2]

This is an open access article under the terms of the Creative Commons Attribution License, which permits use, distribution and reproduction in any medium, provided the original work is properly cited.
© 2022 The Authors. *SPE Polymers* published by Wiley Periodicals LLC on behalf of Society of Plastics Engineers.

fully equipped REESS have to be tested in a fuel fire test. During this fuel fire treatment and for a minimum of 3 h afterwards, the REESS should show no evidence of explosion. To meet these fire retardancy requirements, the fire retardancy of the REESS housing material is of critical importance.

For automotive applications, sandwich structures (SWs) made of thermoplastic-fiber-reinforced face-sheet laminates and thermoplastic-polymer-based cores offer significant potential for weight saving, material performance and cost-efficiency as well as easy recyclability.[3] Several manufacturing methods for thermoplastic SWs are reported in literature, and an overview is provided by Gruenwald et al.[4] Fusion bonding processes using the thermoplastic properties to bond the face sheets to the core are of special interest as no additional adhesives are required.[5] Polypropylene (PP) with glass-fiber (GF) reinforcement in combination with a PP foam core has been one of the most commonly used material combinations for thermoplastic SWs during the last two decades.[3,6,7] Accordingly, much is known about their production and processing methods as well as mechanical performance.

PP is a highly flammable polymer.[8] In order to fulfill fire retardancy requirements, flame retardants (FRs) such as the endothermically active metal hydrates aluminium trihydroxide (ATH) and magnesium hydroxide (MDH), gas-phase-active FRs and char-forming FR systems are incorporated.[8–10] Due to cost-efficiency, metal hydrates are often used for flame-retarded PP materials, whereby the use of MDH ensures the required thermal process stability.[8] Much is reported about the use of flame-retarded PP, for example in wire and cable applications.[8] However, to the best of our knowledge little is reported in the literature about the flame retardancy of PP-GF-EPP SWs.

The aim of this study is therefore to provide detailed insights into the flame retardancy of PP-GF-EPP SWs with regard to application as a housing material for REESS. For this purpose, the flame retardancy of PP-GF tape laminates (TLs) and PP-GF-EPP SWs, both with a variation of the content of the FR MDH as well as the GF content, were studied using the limiting oxygen index (LOI) test, the UL94 test and the cone calorimeter test. Additionally, a bench-scale fuel fire test was used to study the fire behavior of materials based on the requirements of the UNECE-R100-8E test in a material- and cost-efficient way.

2 | EXPERIMENTAL

2.1 | Material processing and sandwich production

For the production of EPP, ARPRO 5195 (PP beads, size: 1.5–3.0 mm, bulk density: 88–102 g/L) from JSP was used. Celstran® CFR-TP PP GF70-13 (PP continuous-fiber [uni-directional] GF-reinforced composite, density: 1660 kg/m^3, 70 wt% E-glass fiber, 0.25 mm tape thickness) from Celanese was used as a tape for the production of FR-free tape laminates. FR-containing tapes were produced from GF TUFROV 4599 (e-glass fiber with silane sizing, roving tex nominal: 2400 g/km, average fiber diameter: 17 µm) from NEG, PP BJ100HP (PP copolymer equipped with an additive package for optimum coupling between polymer matrix and glass fibers, MFR [230 °C/2.16 kg]: 90 g/10 min), density: 904 kg/m^3) from Borealis and the FR $Mg(OH)_2$ ANKERMAG®-H5 from Magnifin. The reference tape laminate (TL Ref) was a GF-PP from ElringKlinger, Germany with a fiber content of 80 wt%.

2.1.1 | Tape production

FR-modified unidirectional continuous-fiber-reinforced PP tapes are produced by melt impregnation. The

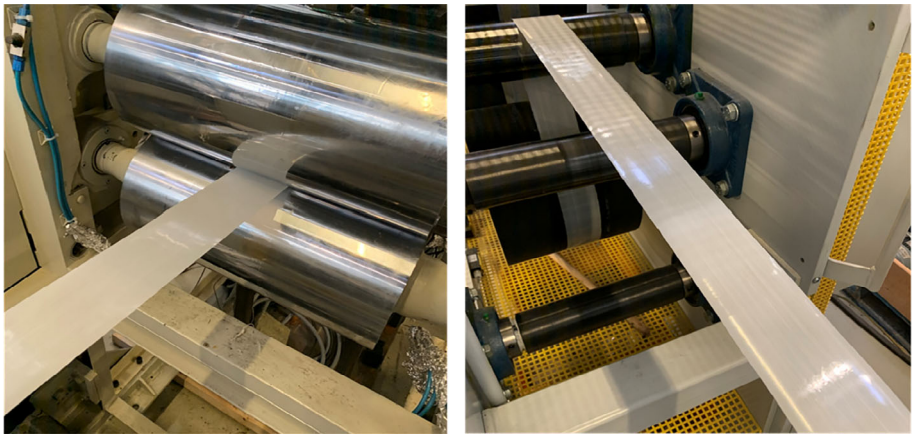

FIGURE 1 Production of T-FR containing 50 wt% FR within PP and 60 wt% GF

TABLE 1 Tapes used in this study

#	Supplier	Fiber content/wt%	MDH content/wt% within PP
T-NFR	Celanese	70	0
T-FR	Self-made	60	50

TABLE 2 TLs of this study

#	FR-containing tape layers	FR-free tape layers
TL (0*-4)	—	4× T-NFR
TL(1*-3)	1× T-FR	3× T-NFR
TL (2*-2)	2× T-FR	2× T-NFR
TL (1*-2–1*)	2× T-FR	2× T-NFR
TL (1*-1–1*-1)	2× T-FR	2× T-NFR
TL (3*-1)	3× T-FR	1× T-NFR
TL (4*-0)	4× T-FR	—
TL Ref	FR-free TL from ElringKlinger	

TABLE 3 SWs produced by fusion bonding

#	FR-containing TL	FR-free TL	Core material
SW (0*-4)	—	TL (0*-4)	EPP
SW (4*-0)	TL (4*-0)	—	EPP
SW Ref	—	TL Ref	EPP

reinforcing GF rovings are pulled off the pay-off creel and fed into a static spreading unit. After passing through the spreading unit, the fibers are pulled through the impregnation die where the thermoplastic melt is brought into contact with the fibers. The impregnated fibers then pass a chill roll system (see Figure 1). The final tape obtained is wound onto a cardboard core for further processing. The tape produced and the tapes used in this study are given in Table 1.

2.1.2 | Tape laminate production

For the production of the tape laminates (TLs) the Fiberforge automated tape laying process (ATL) from Dieffenbacher was used. Four layers of tape with an orientation of 0/90/0/90 were stacked and spot-welded to obtain the predefined lay-ups. For the different combinations within the TLs the following nomenclature is used: TL(x*-x), in which x* is the number of tapes containing FR and *x* is the number of tapes without FR. Furthermore, the chronological order describes the position of the layers within the laminate, for example, TL(1*-3) denotes that the tapes used in first layer (surface of the later produced SW) are flame retarded and layer two to layer four contain no FR.

For the TL production, tapes were cut in length and placed adjacent to each other. Subsequently the lay-ups were consolidated using a radiation-induced vacuum consolidation process (RIVC). This process uses infrared radiation to heat the lay-ups above the melting temperature of the polymer while at the same time a vacuum with an absolute pressure of 1000 Pa is applied. For this purpose, the lay-ups are placed between two IR-transparent tool walls. For thickness calibration, spacers with a cavity size of 500 × 500 mm^2 and a thickness of 1 mm were used. The consolidation temperature was 175 °C. Solidification was achieved using contact cooling. TLs with an area of 400 × 400 mm^2 and a thickness of 1 mm were produced. Table 2 shows the TLs of this study.

2.1.3 | PP bead foam (EPP) production

A 200 kg/m^3 of PP bead foams (EPP) were produced by sintering ARPRO 5195 using an Erlenbach - EHV 670/570 steam chest molding unit with a 500 × 500 × 10 mm^3 tool. The EPP is dried at 80 °C for 4 h before further processing by hot wire cutting into 400 × 400 × 10 mm^3 plates.

2.1.4 | Sandwich production by fusion bonding

SWs were produced by a modified RIVC process. 400 × 400 × 1 mm^3 tapes were placed above and below an EPP core of 400 × 400 × 10 mm^3. The fiber orientations of the tapes were mirrored to the sandwich core. The SWs were produced at a vacuum pressure of 80 kPa and a joining temperature of 150 °C using 12 mm spacers (see Table 3, Figures 2 and 3).

2.2 | Characterization

Test specimens were obtained by wet abrasive grinding using a MS200 cutting machine from Vibrationstechnik, Germany.

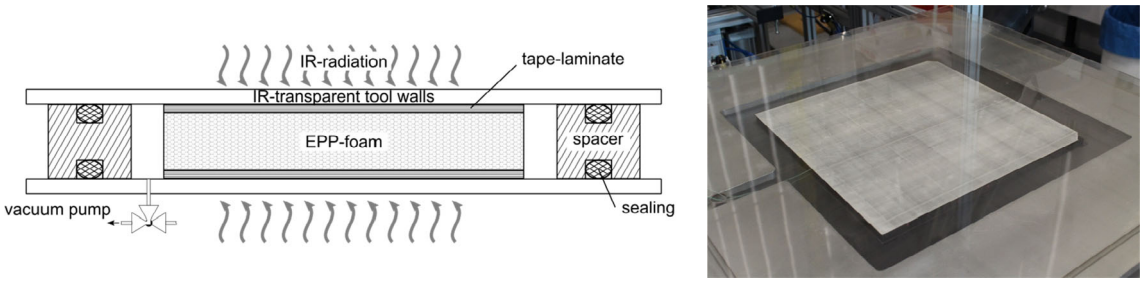

FIGURE 2 Sandwich production by fusion bonding. Left: Process diagram; Right: SW plate

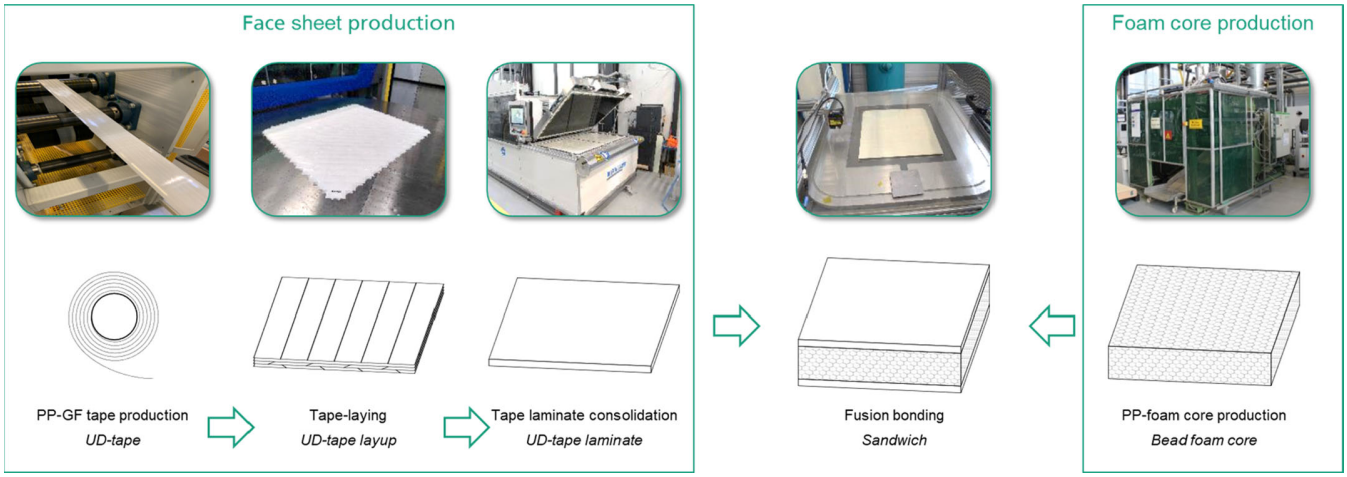

FIGURE 3 Sandwich production – Process overview

2.2.1 | Limiting oxygen index

The LOI value was measured using an oxygen index module from FIRE according to DIN EN ISO 4589-2 standardized procedure. The sample size was type III ($80 \times 10 \times 1\ mm^3$).

2.2.2 | UL94

The UL94 V test was performed with a UL94 Test Device from WAZAU, Germany according to the UL94 standard using $13 \times 125 \times 3\ mm^3$ samples. In the UL94 test, a 50 W Bunsen burner is applied two times for 10 s each on a test specimen.

2.2.3 | Cone calorimeter ISO 5660-1

Cone calorimeter measurements were taken using an ISO 5660-1 device from WAZAU. The sample size was $100 \times 100\ mm^2$ (thickness depending on plate or sandwich thickness), with three samples tested for each material. The samples were wrapped in aluminium foil and positioned horizontally at a distance of 25 mm from the cone base heater plate, where a heat flux of $35\ kW/m^2$ was applied. The data were recorded in increments of 1 s.

2.2.4 | Bench-scale fuel fire test

A laboratory flammability test stand developed by Rüttgers Organic GmbH to test intumescent coatings was modified using a $170 \times 170\ mm^2$ steel pan filled with 60 ml of petrol (Super 95 E5, DIN EN 228, ROZ 95) to create a fuel fire for about 120–130 s. The distance between the steel pan and the surface of the test specimen was about 300 mm. $190 \times 190\ mm^2$ test specimens, mounted on a steel test specimen holder, were used. The temperature of the reverse side of the test specimen was measured by a surface thermo probe (K type, measurement range −50 °C to +650 °C) from B & B Thermo-Technik and recorded in increments of 1 s. Figure 4 shows the bench-scale fuel fire test bench.

3 | RESULTS AND DISCUSSION

3.1 | Flame retardancy of PP-GF tape laminates (TLs)

PP-GF TLs form the cover layers of the SW. In the event of a fire, the external TLs are the first to be affected directly by the fire and heat. To study the influence of flame-retarded tape layers containing the FR MDH on the flame retardancy of a TL containing four tape layers, tape layers with different layer structures were tested.

Table 4 shows the LOI and UL94 test results of the PP-GF TLs. The flame retardancy of the TL increases, indicated by a rising LOI value, with increasing numbers of flame-retarded tapes. However, the LOI value of TL (4*-0), which contains four flame-retarded tapes, is lower than that of TLs containing three or two flame-retarded layers. Unexpectedly, TL (1*-2–1*) and TL (1*-1–1*-1) show the highest LOI values.

During the LOI test, a loss of structural integrity is observed. After the polymer is pyrolyzed, the individual fibers are visible. The fibers no longer stick together and fan out. The PP polymer matrix pyrolyzes completely and the remaining GFs lose their integrity. It is assumed that the remaining FR exacerbates this loss of structural integrity, whereas FR-free tape layers enhance the structural integrity. TL (4*-0) therefore shows a lower LOI value than TL (3*-1) and TL (2*-2), and the TLs with alternating tape layer structures TL (1*-2–1*) and TL (1*-1–1*-1) show the highest flame retardancy.

The loss of structural integrity is also observed during the vertical UL94 test. In the UL94 test, the PP polymer matrix is pyrolyzed completely, whereby the remaining GF structure falls apart. All TLs fail the UL94 test. The UL94 test set-up is currently often used for the development of materials for REESS. However, it is assumed that neither the UL94 test set-up nor the LOI test set-up are suitable to develop and investigate the flame retardancy of REESS materials, especially REESS made of thermoplastic material.

Besides the LOI and UL94 tests, cone calorimetry tests were performed. Table 5 shows the results of the cone calorimetry tests on the PP-GF TLs. In contrast to flame treatment parallel to the specimen cross-section as in the LOI and UL94 test, the heat treatment of the cone heater occurs on the surface of the PP-GF TL. Due to the horizontal test set-up, a loss of structural integrity caused by polymer pyrolysis as well as the detachment, fan out and falling off of the exposed fibers is minimized.

Time to ignition (TTI) and time of afterflame (Afterflame) of the TLs are slightly increased by flame-retarded layers but do not change when different numbers of flame-retarded layers are used. However, the peak heat release rate (pHRR), the total heat release (THR) and the total smoke release (TSR) decrease significantly with increasing numbers of flame-retarded tape layers. Considering all three of these measures, TL (3*-1), with three flame-retarded layers, shows a significantly improved flame retardancy. Compared to the FR-free TL (0–4*), TL (3*-1) reduces the pHRR by 54%, the THR by 26% and the TSR by 25%. The completely flame-retarded TL (4*-0) improves the flame retardancy some more by reducing the pHRR by 59%, the THR by 36% and the TSR by 44%. Based on the HRR curves of the TLs given in Figure 5, three main observations are made:

TABLE 4 LOI and UL94 test results of the PP-GF tape laminates (TLs)

#	LOI/O_2%	UL94 results
TL (0*-4)	19.1 ± 0.38	n.c.
TL (1*-3)	20.1 ± 0.38	n.c.
TL (2*-2)	21.4 ± 0.38	n.c.
TL (1*-2–1*)	22.1 ± 0.38	n.c.
TL (1*-1–1*-1)	24.6 ± 0.38	n.c.
TL (3*-1)	21.9 ± 0.38	n.c.
TL (4*-0)	20.8 ± 0.27	n.c.
TL Ref	20.9 ± 0.38	n.c.

Note: n.c., not classified by the UL94 test due to strong burning.

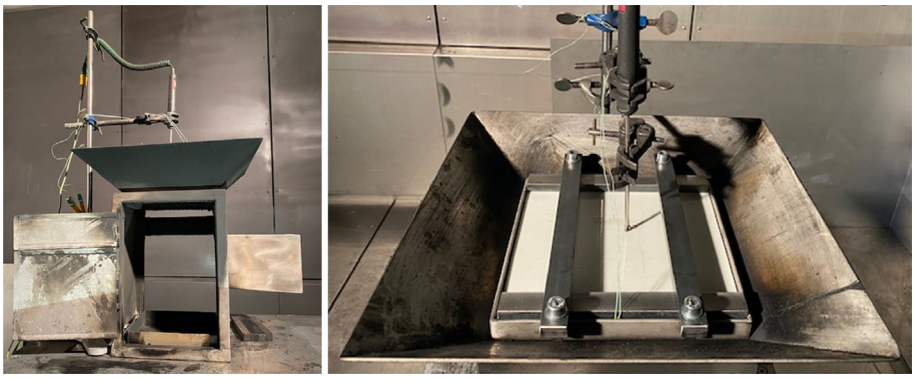

FIGURE 4 Bench-scale fuel fire test bench. Left: Test bench; Right: Test specimen (SW with additional internal thermocouples) mounted into a steel test specimen holder

TABLE 5 Cone calorimetry test results of the PP-GF tape laminates (TLs); FR-containing layer(s) of the TL are oriented to the cone heater (cone heat flux of 35 kW/m^2)

#	TTI/s	Afterflame/s	pHRR/kW/m^2	Time of pHRR/s	THR/MJ/m^2	TSR/m^2/m^2	Residue/%
TL (0*-4)	34 ± 2	272 ± 59	312 ± 5	78	19.9 ± 0.5	124 ± 16	69.0 ± 0.7
TL (1*-3)	40 ± 1	236 ± 72	314 ± 5	104	17.8 ± 0.5	111 ± 19	71.1 ± 0.4
TL (2*-2)	40 ± 3	264 ± 49	224 ± 25	117	15.2 ± 0.4	116 ± 31	71.7 ± 1.2
TL (3*-1)	39 ± 3	296 ± 74	143 ± 7	plateau	14.7 ± 0.7	93 ± 19	71.7 ± 1.7
TL (4*-0)	41 ± 3	252 ± 6	128 ± 4	plateau	12.8 ± 0.2	69 ± 34	74.6 ± 2.0
TL Ref	33 ± 4	215 ± 31	245 ± 9	63	14.0 ± 1.0	102 ± 8	78.0 ± 0.8

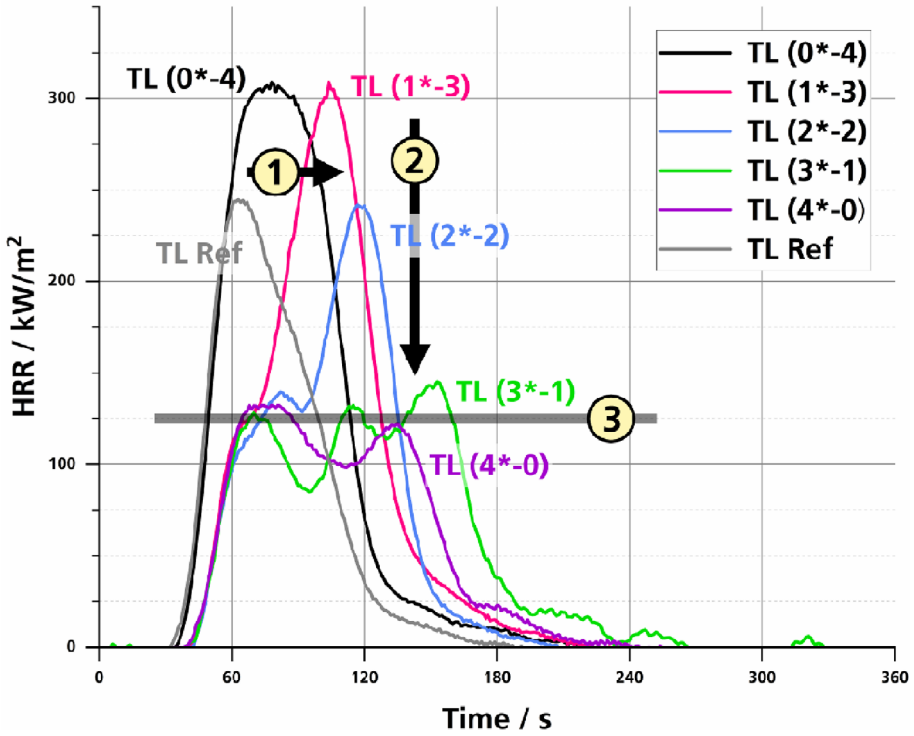

FIGURE 5 Comparison of heat release rate (HRR) measurements of PP-GF tape laminates (TLs) and effect of FR layers; **1**: Increase of the time needed to reach pHRR, **2**: Reduction of the HRR, **3**: HRR plateau formation (125 kW/m^2 marker)

1. **Increase of the time needed to reach pHRR:** The time needed to reach pHRR increases with increasing numbers of flame-retarded tape layers of the TL. The time of pHRR is 78 s for the FR-free TL (0*-4) and increases to 104 s for TL (1*-3), and 117 s for TL (2*-2). TL (3*-1) and TL (4*-0) show no pHRR. Rather, a pHRR plateau of about 125 kW/m^2 is observed in the time interval from 65 s to 160 s. It is assumed that a stepwise pyrolysis of the tape layer takes place. Due to the reduced amount of pyrolyzable polymer material within the flame-retarded tape layers, the pHRR is observed as soon as the FR-free tape layer starts to thermally decompose. With increasing numbers of flame-retarded tape layers on top of the FR-free tape layers, the time needed to reach the pHRR increases.
2. **Reduction of the pHRR:** A reduction of the pHRR is observed with increasing numbers of flame-retarded tape layers of the TL. Both TL (0*-4) and TL (1*-3) show a pHRR of about 313 kW/m^2. Two flame-retarded layers lead to a pHRR of 224 kW/m^2 (TL [2*-2]). TL (3*-1) and TL (4*-0) show a HRR plateau of about 125 kW/m^2. The amount of FR, as well as FR effects and the resulting lower content of PP, are responsible for these observations.
3. **HRR plateau formation:** The formation of a HRR plateau at about 125 kW/m^2 is observed with increasing numbers of flame-retarded tape layers in the TL. TL (1*-3) with one flame-retarded layer shows a weak local shoulder at about 70 s. For TL (2*-2), a local maximum is observed at 82 s. TL (3*-1) and TL (4*-0) show an overall HRR plateau in the time interval from 65 s to 160 s with two or three local maxima. Based on these results, a TL with a four-tape layer, consisting of three flame-retarded tape layers, seems

sufficient to suppress the occurrence of a HRR peak. The formation of a HRR plateau is typical for a thermally thick charring material.[11] As the FR-free laminate shows no HRR plateau but only a single HRR peak, a normal combustion reaction of the PP polymer of all four layers is assumed. By the incorporation of FR-containing tape layers, thermal barrier layers are formed during the burning process. The formation of a HRR plateau with several local maxima indicates for each local minimum the formation and for each peak the successive destruction of thermal barrier layers.

Similar observations are made for the reference material TL Ref. The time needed to reach the pHRR is not reduced. Instead, the pHRR of TL Ref is observed 15 s earlier (at 63 s) than that of the FR-free TL (0*-4). Due to the higher a GF content and the lower amount of flammable polymer material, the pHHR and the THR of TL Ref are lower than the pHRR and THR of TL (0*-4). TL Ref shows no plateau formation as no flame-retarded tape layers are incorporated.

3.2 | Flammability of the sandwich structures

To investigate the flame retardancy of PP-GF-EPP SW, three different SWs are used - one SW with FR-free TLs (TL (0*-4)), one SW with fully flame-retarded TLs (TL (4*-0)) and one SW with increased GF content (TL Ref). Table 6 shows the LOI and UL94 test results. The EPP foam core dominates the flaming behavior of the LOI and UL94 test specimen. A slight increase of the LOI value from 18.3 O_2% to about 19.4 O_2% is observed for the SW structures compared to the TL-free EPP foam. However, the use of flame-retarded TLs as well as the use of a higher amount of GF (TL Ref) do not influence the LOI value. Due to the vertical test flame set-up of the UL94 test with flame penetration of the SW cross section, none of the SW specimens passed the UL94 test. As already mentioned, it is assumed that neither the UL94 test set-up nor the LOI test set-up are suitable to investigate the flame retardancy of REESS materials.

The results of the cone calorimeter test with heat treatment of the specimen surface of EPP and of the SWs are shown in Table 7. Compared to the TLs, EPP foam shows complete pyrolysis with a short TTI of 15 s and a high pHRR of 626 kW/m^2.

Figure 6 shows the HRR measurements of the PP-GF-EPP SWs.

Based on the HRR curves, the following main effects caused by the flame-retarded TLs are observed:

TABLE 6 LOI and UL94 test results of the PP-GF-EPP sandwich structures (SWs)

#	LOI/O_2%	UL94 results
EPP	18.3 ± 0.27	n.c.
SW (0*-4)	19.3 ± 0.27	n.c.
SW (4*-0)	19.5 ± 0.40	n.c.
SW Ref	19.3 ± 0.48	n.c.

Note: n.c., not classified by the UL94 test due to strong burning.

1. **Increase of TTI:** Due to the use of flame-retarded TLs, the TTI observed for SW (4*-0) increases by 13 s (32%). An increase of TTI due to flame-retarded TLs was already observed in the cone calorimeter measurement of the TLs.
2. **Reduction of the pHRR of the external surface TL:** The pHRR of the external surface TL (first local maximum) is 230 ± 15 kW/m^2 for SW (0*-4) and 99 ± 9 kW/m^2 for the flame-retarded SW (4*-0). The reduction of the pHRR of the external surface TL is about 57% (131 kW/m^2). This effect is similar to the reduction of the pHRR of the TLs which is about 59% for TL (4*-0) compared to TL (0*-4). However, no stepwise decomposition with two to three peaks and no formation of a peak plateau are observed for the thermal decomposition of the external surface layer of SW (4*-0). It is assumed that the thermal decomposition of the lower TL layers and the EPP occurs at the same time. The external TL of SW (4*-0) decomposes with one single decomposition peak with a peak shoulder. It is assumed that the thermal insulating effect and the beginning of the decomposition of the EPP foam core is responsible for this effect.
3. **Increase of TTI of the EPP foam core:** The flame-retarded TL affects the thermal decomposition of the EPP. The local HRR minimum between the pHRR of the external surface TL and the pHRR of the EPP foam core is 157 ± 25 s for SW (0*-4) and 164 ± 18 s for SW (4*-0). However, the following HRR rise seems to be more meaningful, for example, exceeding the 125 kW/m^2 HRR value (plateau of TL (4*-0)) after the pHRR of the external surface TL. SW (0*-4) exceeds the 125 kW/m^2 HRR value at 199 ± 22 s whereas SW (4*-0) exceeds this value about 2 min later at 331 ± 10 s (+66%).
4. **Reduction of the pHRR:** Due to the use of flame-retarded TLs, the pHRR for SW (4*-0) is reduced by 38 kW/m^2 (13%).

Beside these effects, the observed THR of SW (0*-4) is slightly (6.5 MJ/m^2) lower than the sum of the THR of EPP and two times the THR of TL (0*-4) (total:

TABLE 7 Cone calorimetry test results of the PP-GF-EPP sandwich structures (SWs)

#	TTI/s	Afterflame/s	pHRR/kW/m²	THR/MJ/m²	TSR/m²/m²	Residue/%
EPP	15 ± 3	425 ± 57	626 ± 34	76.0 ± 3.3	656 ± 44	0.7 ± 0.9
SW (0*-4)	41 ± 7	846 ± 91	291 ± 40	109.3 ± 3.8	1169 ± 93	47.2 ± 0.8
SW (4*-0)	54 ± 7	1081 ± 80	253 ± 29	107.7 ± 2.4	1066 ± 240	44.8 ± 0.7
SW Ref	38 ± 2	869 ± 101	284 ± 28	104.5 ± 1.2	1154 ± 82	50.4 ± 0.4

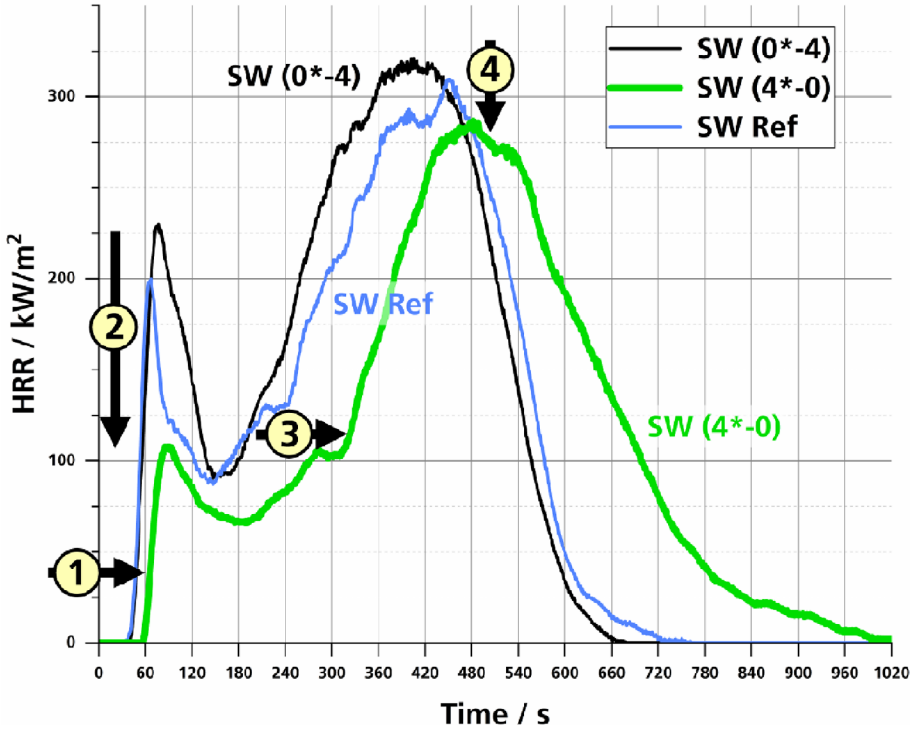

FIGURE 6 Comparison of heat release rate (HRR) measurements of PP-GF-EPP SWs and the effect of FR layers; **1**/**2**: Increase of TTI and reduction of the pHRR of the external surface TL; **3**/**4**: Increase of TTI and reduction of the pHRR of the EPP foam core

115.8 MJ/m²), whereas the observed THR of flame-retarded SW (4*-0) is slightly (6.1 MJ/m²) higher than the sum of the THR of EPP and two times THR of TL (4*-0) (total: 101.6 MJ/m²). It is assumed that the TL of the external surface (oriented to the cone heater) decomposes completely due to the burning EPP (increase of the THR of SW (4*-0)). The THR, the TSR and the residue of SW (0*-4) and SW (4*-0) are of the same order of magnitude.

In comparison to SW (0*-4), the SW Ref material with a higher amount of GF shows an earlier TTI, a slightly lower pHRR for the external surface TL as well as for the EPP foam core, and a similar THR and TSR. The TTI of the enclosed EPP foam core is increased.

3.3 | Bench-scale fuel fire test

PP-GF-EPP SWs are of interest for applications as housings for REESS of electric vehicles. The UNECE Regulation No. 100 Annex 8E - Fire Resistance[2] (UNECE-R100-8E) describes the fire resistance test which has to be passed by REESS used in a vehicle. It simulates a fuel fire from outside of a vehicle flaming the REESS. In the UNECE-R100-8E test, a fuel fire is applied to the REESS for about 130 s. Test criterion: During this fuel fire treatment and for a minimum of 3 h afterwards, the REESS must show no evidence of explosion.

For the development of REESS housing materials and related processing, the test of a fully equipped REESS for each material and process configuration is too costly in terms of use of material and production effort. A bench-scale fuel fire test was therefore used to simulate the fire behavior of materials based on the UNECE-R100-8E test. In this bench-scale fire test, a fuel fire of commercial petrol was applied for 120–130 s to test specimens made from TLs and SW plates. To prevent a deformation, which could cause the specimen to fall into the fuel pan during the test, the test specimens were fixed in a steel frame. This test set-up is not validated for the UNECE-R100-8E test, but allows the investigation of several important burning characteristics of the specimens:

TABLE 8 Bench-scale fuel fire test results of PP-GF tape laminates (TL)

#	Reverse side ignited	Mass loss/%	$T_{max,reverse\ side}$/°C	t of T_{max}/s
TL (0*-4) a	Yes (after 79 s)	25.6	480.5	79
TL (0*-4) b	No	21.8	484.4	84
TL (1*-3) a	Yes (after 80 s)	24.4	454.3	80
TL (1*-3) b	Yes (after 76 s)	22.2	474.7	76
TL (2*-2) a	No	17.8	457.2	91
TL (2*-2) b	No	19.2	477.6	95
TL (1*-2–1*) a	No	15.3	501.8	91
TL (1*-2–1*) b	No	15.1	510.5	92
TL (1*-1–1*-1) a	No	14.4	433.9	102
TL (1*-1–1*-1) b	No	14.5	401.7	88
TL (3*-1) a	No	16.3	441.7	103
TL (3*-1) b	No	16.6	497.9	88
TL (4*-0) a	No	18.9	498.9	95
TL (4*-0) b	No	18.8	500.8	94
TL Ref	No	16.1	503.7	88
TL Ref	No	16.0	516.3	83
EPP	Yes (after 68 s)	100	189.9	68

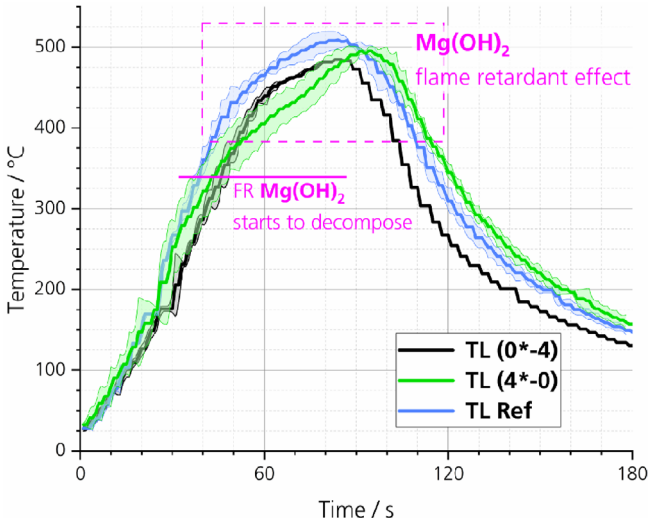

FIGURE 7 Temperature profile (mean value) of the specimen reverse side of TL (0*-4), TL (4*-0) and TL ref measured by the bench-scale fuel fire test

1. **Self-extinction:** Self-extinction of the specimen indicates whether the material is able to extinguish by itself or if the material continues to burn after the 120–130 s fuel fire treatment. An open fire near a damaged and thermally treated REESS is a risk. Gases generated from components in the REESS, which can be flammable, are released by the damaged REESS structure or intentionally by the pressure relief valve of the REESS. For this reason, materials with low afterflame time or self-extinction properties are preferable.
2. **Ignition of the reverse side of the specimen:** The test set-up of the bench-scale fuel fire test does not allow an easy ignition of pyrolysis gases released from the reverse side of the specimen. Ignition of the back of the sample therefore indicates that the flame has penetrated the sample from the fire side. To protect the critical components, systems and sensors inside the REESS from fire, REESS housing materials should not show any breakthrough of the flame, and therefore in the bench-scale fuel fire test no ignition should occur on the reverse side of the specimen.
3. **Structural integrity:** Material used for REESS housing should retain their structural integrity during and after the fuel fire treatment. Especially the entire disintegration (e.g., formation of holes) of the material should be prevented. However, actual mechanical stress of the REESS during the UNECE-R100-8E test (e.g., pressure from the inside of the REESS) is not represented by the bench-scale test set-up.
4. **Mass loss:** The mass loss indicates how much material is lost by both the decomposition of the material, dripping (for example from molten parts), and the dropping off of looser char layers or GFs. It also indicates the formation of protective layers, for example caused by a FR, and the protection against degradation and decomposition of the deeper layer.

TABLE 9 Bench-scale fuel fire test results of PP-GF-EPP sandwich structures (SWs)

#	Mass loss/%	$T_{max,reverse\ side}$/°C	t of T_{max}/s
SW (0*-4) a	5.6	80.2	357
SW (0*-4) b	5.9	86.8	315
SW (0*-4) c	6.1	83.4	323
∅	5.9 ± 0.25	83 ± 3.3	332 ± 22
SW (4*-0) a	4.5	80.3	383
SW (4*-0) b	4.7	72.7	375
SW (4*-0) c	4.7	76.8	389
∅	4.6 ± 0.12	77 ± 3.8	382 ± 7
SW Ref a	4.4	88.0	338
SW Ref b	4.5	85.8	325
SW Ref c	4.5	78.8	308
∅	4.5 ± 0.6	84 ± 4.8	324 ± 15

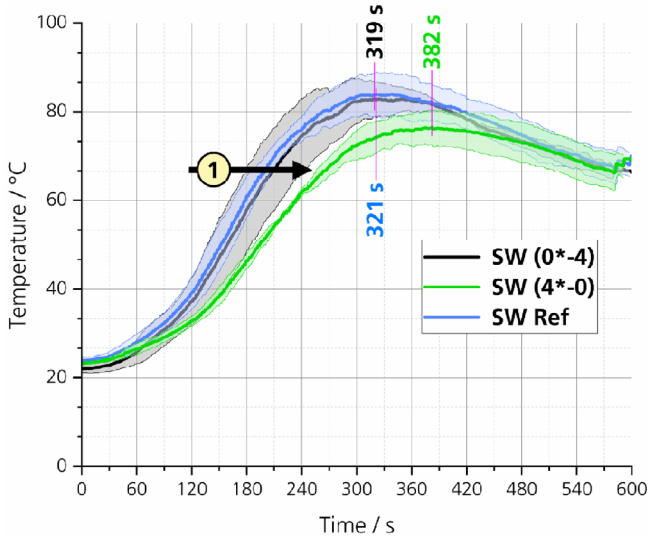

FIGURE 8 Temperature profile (mean value) of the specimen reverse side of SW (0*-4), SW (4*-0) and SW ref measured by the bench-scale fuel fire test. **1**: Delay of the reverse side temperature rise

5. **Temperature of the reverse side of the specimen:** The inside temperature of a REESS is of particular importance. If the battery cells of the REESS become too hot, a thermal-runaway of the REESS can be triggered. It is assumed that an inside temperature above 80 °C leads to irreversible damage of the cells for example, by the decomposition of the electrolyte. Above 120 °C, the release of decomposition gases occurs and the thermal-runaway is most likely triggered. Since it must be assumed that the temperature control systems of the REESS are damaged and offline during a real fire (post-car-accident fire), the temperature of the reverse side of the specimen should be as low as possible. It is assumed that this temperature should under no circumstances exceed the boiling point of the REESS liquids, especially that of the often flammable electrolyte.

Table 8 shows the bench-scale fuel fire test results of the TLs and EPP foam. Two specimens were tested from each material. The EPP foam burns completely. After 68 s, the fuel fire breaks through the EPP specimen and ignites the reverse side of the specimen. At this moment, the specimen reverse side temperature is 190 °C. Of all the TLs, only the FR-free TL (0*-4) and TL (1*-3) with one FR-containing tape layer show a fuel fire breakthrough. TLs with two, three or four flame-retarded tape layers resist the fuel fire.

As regards the mass loss of the TL, a decrease occurs when the number of flame-retarded tape layers is increased to one and two. However, the TLs containing three and four flame-retarded tape layers show a mass loss increase in comparison to the TLs with two flame-retarded tape layers. The lowest mass loss of 14.4 ± 0.1% is observed for TL (1*-1–1*-1). TL (1*-1–1*-1) also shows the lowest temperature maximum of the specimen reverse side of 418 ± 16°C. The $T_{max,reverse\ side}$ of the other TLs is in the range of 442–511 °C. As already described for the LOI value, TL (1*-1–1*-1) shows the highest LOI value/flame retardancy, and it is assumed that the FR-free tape layers enhance the structural integrity of the TL during the burning process.

Figure 7 shows the temperature profile of the specimen reverse side of TL (0*-4), TL (4*-0) and TL Ref. Compared to the FR-free TL (0*-4), the fully flame-retarded TL (4*-0) shows a delayed temperature increase above

TABLE 10 Bench-scale fuel fire test results of PP-GF-EPP sandwich structures (SWs) equipped with additional thermocouples between the external surface layer and the EPP foam core (T_1) and between the EPP foam core and the TL of the reverse side (T_2)

#	Afterflame/s	Mass loss/%	$T_{max,1}$/°C ($t_{max,1}$/s)	$T_{max,2}$/°C ($t_{max,2}$/s)	$T_{max,reverse\ side}$/°C ($t_{max,reverse\ side}$/s)
SW (0*-4) a	36	6.3	347.4 (102)	signal lost	75.7 (338)
SW (0*-4) b	33	6.6	449.4 (112)	109.3 (340)	79.5 (341)
SW (0*-4) c	24	6.9	412.4 (101)	109.0 (313)	80.5 (315)
SW (0*-4) d	19	6.9	393.9 (97)	107.9 (314)	80.2 (326)
∅	28 ± 7.9	6.7 ± 0.29	401 ± 42 (103 ± 6)	109 ± 0.7 (322 ± 15)	79 ± 2.2 (330 ± 12)
SW (4*-0) a	14	4.4	420.2 (109)	99.5 (350)	76.2 (387)
SW (4*-0) b	4	4.9	430.0 (109)	104.8 (361)	80.1 (370)
SW (4*-0) c	3	4.9	339.8 (112)	100.9 (362)	78.4 (396)
SW (4*-0) d	11	4.6	335.9 (106)	107.5 (347)	82.7 (365)
∅	8 ± 5.4	4.7 ± 0.24	381 ± 51 (109 ± 2)	103 ± 3.7 (355 ± 8)	79 ± 2.7 (380 ± 14)

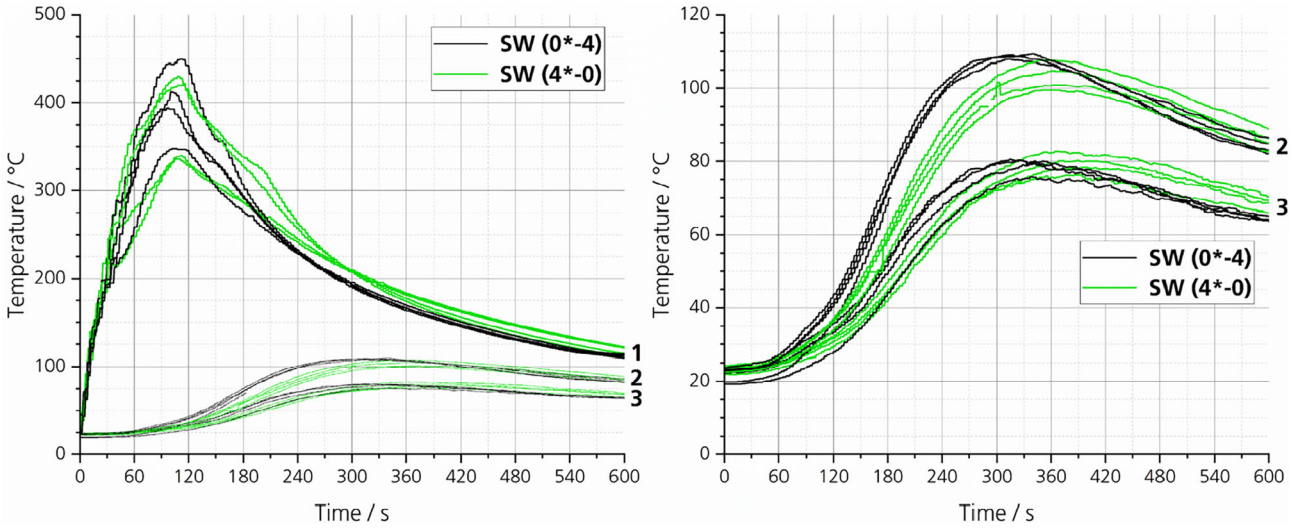

FIGURE 9 Right: Temperature profiles of the thermocouples between the TL exposed to fire and the EPP foam core (**1**), between the EPP foam core and the TL of the reverse side of the SW (**2**) and at the reverse side of the SW (**3**) measured for SW (0*-4) and SW (4*-0) in the bench-scale fuel fire test. Left: Enlargement of the temperature profiles of thermocouple (**2**) and thermocouple (**3**)

375°C. TL (4*-0) reaches the $T_{max,reverse\ side}$ about 13 s (after 95 ± 1 s) later than TL (0*-4). The intended effect of a delayed temperature rise is achieved by using the FR MDH. It is assumed that a flame-retardant effect of MDH by cooling caused by endothermic decomposition is responsible for this. However, the observed $T_{max,reverse\ side}$ of TL (4*-0) with 500 ± 1 °C is 17 °C higher than the $T_{max,reverse\ side}$ of TL (0*-4). Compared to TL (0*-4), TL Ref initially heats up faster at temperatures above 375 °C. $T_{max,reverse\ side}$, however, is reached at the same time as for TL (0*-4). The $T_{max,reverse\ side}$ of 510 ± 6 °C of TL Ref is the highest of all tested TLs. Based on these observations, a higher content of inorganic and thermally stable materials like GFs (TL Ref) and MDH (TL (0*-4)) leads to higher $T_{max,reverse\ side}$.

The increase of the inside wall temperature of the housing material to about 500 °C within 90 s seems to be a major risk for the REESS. However, TLs are not supposed to be used without a core material for structural parts like the housing of a REESS. Nevertheless, the core material must withstand this high-temperature treatment. A slow temperature rise and a low T_{max} of the reverse side are preferable. Especially for the slower temperature rise, the fully flame-retardant TL (4*-0) has a slight advantage.

The bench-scale fire test results of three specimens each from the FR-free SW (0*-4), the FR MDH- containing SW (4*-0) and the reference SW Ref are shown in Table 9 and Figure 8. For all three SWs, a low maximum temperature of the test specimen reverse side in the range

of 70–90 °C is observed. The flame-retarded tape layer containing SW (4*-0) shows the lowest $T_{max,reverse\ side}$ of 76.6 ± 3.8 °C. This temperature is reached after 382 ± 7 s, which is about 51 s later than SW (0*-4). The intended effects of a delayed temperature rise and a lower $T_{max,reverse\ side}$ are achieved using the FR MDH.

In comparison to SW (0*-4), SW Ref shows no differences in $T_{max,reverse\ side}$ which is 84.2 ± 4.8 °C and in the time this temperature is reached which is 324 ± 15 s. The GF content of the TLs therefore seems to have a slight influence on the overall fire behavior of the SWs.

A lower mass loss is observed for both SW (4*-0) and SW Ref due to the reduced overall amount of PP. Based on these observations, the incorporation of a FR into the SW structure is more efficient to lower the inside temperature of a REESS in the event of an external fire than an increase of the fiber content or a decrease of the flammable polymer content. The temperature inside the REESS also rises more slowly for the flame-retarded SW (4*-0), as indicated by Figure 8 (marking 1). In the event of an external fire, heat control systems inside the REESS (if functional) are able to dissipate thermal energy for a longer period. The increase in the inner wall temperature of the housing material to 90 °C within 5 min observed for SW (0*-4) and SW Ref should, however, also represent a low risk for the REESS.

To measure the inside temperatures of the SWs during the fuel fire treatment, SWs were equipped with two fine thermocouples within the sandwich melt-joining process. One thermocouple is located between the TL exposed to the fuel fire and the EPP foam core, and the other between the EPP foam core and the TL on the SW reverse side. The measurement point of both thermocouples is in the center of the SW plate. Table 10 and Figure 9 show the bench-scale fuel fire test results of SW (0*-4) and SW (4*-0). Four specimens of each material were tested.

The observed maximum temperature of each thermocouple is of the same order of magnitude for both the FR-free SW (0*-4) and the fully flame-retarded SW (4*-0). For SW (0*-4), average values of $T_{max,1}$: 401 ± 42 °C, $T_{max,2}$: 109 ± 0.7 °C and $T_{max,reverse\ side}$: 79 ± 2.2 °C are observed. For the fully flame-retarded SW (4*-0) a $T_{max,1}$: 381 ± 51 °C, $T_{max,2}$: 103 ± 3.7 °C and $T_{max,reverse\ side}$: 79 ± 2.7 °C are measured. Especially the $T_{max,2}$ of the thermocouples between the EPP foam core and the TL of the reverse side (T_2) show the thermal insulation capability of the EPP foam even during the fire. As is clear from the standard deviations, the measured values of the thermocouple between the TL exposed to fire and the EPP foam core (T_1) vary greatly and are prone to errors, since the signal or material contact is lost.

However, the temperature rise is slower in case of the flame-retarded SW (4*-0). SW (4*-0) reaches $T_{max,1}$ after 109 ± 2.4 s, $T_{max,2}$ after 355 ± 7.6 s and $T_{max,reverse\ side}$ after 380 ± 14.5 s, whereas the FR-free SW (0*-4) reaches $T_{max,1}$ after 103 ± 6.4 s, $T_{max,2}$: after 322 ± 15.3 s and $T_{max,reverse\ side}$ after 330 ± 11.9 s.

In addition to the less favorable temperature rise behavior, the FR-free SW (0*-4) shows a reduced self-extinction indicated by an afterflame of about 19–36 s. In contrast, the flame-retarded SW (4*-0) extinguishes after 3–14 s. A correlation between T_{max} and the time of afterflame is not observed.

As expected, the mass loss of SW (0*-4) is higher than the mass loss of SW (4*-0).

4 | CONCLUSIONS

In this study, the flame retardancy of continuous-GF-reinforced PP (PP-GF) tape laminates (TLs) with different structures of the four-tape layers - used also in SWs containing two PP-GF TLs and one PP bead foam core (PP-GF-EPP SW) - are investigated by LOI, UL94, cone calorimeter tests and a bench-scale fuel fire test. Three SWs are investigated - one SW with FR-free TLs, one SW with fully flame-retarded TLs (FR: $Mg(OH)_2$) and one SW with increased GF content. These SWs are intended for use as housing materials for rechargeable energy storage systems (REESS) in electric vehicles.

The LOI and UL94 tests do not provide clear information regarding the burning behavior of the material during a post-car-accident fire scenario, because in the LOI and UL94 test the edge of the test specimen is treated. In a real car-accident fire, typically the entire housing (surface area) of the REESS is exposed to the fire. In particular, the lateral and non-planar arrangement of the test specimen and the fibers it contains relative to the flame results in high flammability and a significant loss of integrity of the test specimen due to fan out of the GFs during the test. In a post-car-accident fire, the housing and the interior continuous-fiber reinforcement is located in a planar position above the fire, which prevents the loss of integrity by fan out of the fibers.

Cone calorimetry tests show that the incorporation of three flame-retarded tape layers in a four-tape-layer TL is already sufficient to suppress the occurrence of a HRR peak, and reduces the pHRR by 54%, the THR by 26% and the TSR by 25%. A fully flame-retarded TL reduces the flammability even more. For the three SW materials, four major observations can be made where fully flame-retarded TLs are used. (a) the TTI is increased by 32%; (b) the pHRR of the external surface of the TL is reduced by 57%; (c) the TTI of the EPP foam core (125 kW/m^2

HRR marker - see Figure 5) is increased by 66%; and (d) the pHRR of the EPP foam decomposition is reduced by 13%. In comparison, the use of TLs with a higher amount of GF (SW Ref) instead of FR results in fewer improvements in flame retardancy. Based on the cone calorimeter test results, SWs with fully flame-retarded TLs are preferable to SWs with TLs containing a higher GF amount.

In the bench-scale fuel fire test, which was designed to simulate the UNECE-R100-8E test on a small scale, TLs containing the FR MDH or an increased GF content show improved fire retardancy. For all three tested SWs, a low maximum temperature of the reverse side of the test specimen, in the range of 70–90 °C, is observed. However, the SW with fully flame-retarded TLs shows a lower temperature rise and a shorter time of afterflame. Future work must show to what extent the results of the bench-scale fuel test correlate with those of the UNECE-R100-8E.

Material selection for a REESS to be further investigated: Incorporating the FR $Mg(OH)_2$ into the TLs of a PP-GF-EPP SW structure should be more efficient in lowering the internal temperature when used for a REESS in the event of an external fire than increasing the amount of GF in the TL. In particular, the temperature inside the REESS should rise more slowly for the flame-retarded SW. In the event of an external fire, heat control systems inside the REESS (if functional) could more easily dissipate thermal energy. The rise of the inside wall temperature of the housing material to a maximum of 90 °C within 5 min, as is observed for the FR-free SW and SW Ref with a higher amount of GF, should, however, also pose a low risk to a REESS and the battery cells. The improved self-extinction of the flame-retarded SW structure increases the safety for surrounding components and reduces the risk of igniting leaking gases.

Further work will show how these components actually behave in the UNECE-R100-8E test when the TL and SW are used in REESS systems.

ACKNOWLEDGMENTS

The authors would like to thank their colleagues at Fraunhofer ICT, Pfinztal: Benedikt Bitzer, Michael Abert, Volker Weiser, Armin Keßler, Sebastian Knapp, Fabian Frank, Johannes Liebertseder, Michael Holzapfel, Michael Weinert and Paul Müller for technical and analytical support, as well as their colleagues from Fraunhofer LBF, Darmstadt: Philipp Kukla and Michael Großhauser for the cone calorimeter measurements. The polymer and additive suppliers are gratefully acknowledged for the provision of all material. The authors especially thank ElringKlinger for providing the reference material and for fruitful discussions. Financial support was provided by the Fraunhofer-Gesellschaft within the Fraunhofer project Light Materials 4 Mobility. Open Access funding enabled and organized by Projekt DEAL.

DATA AVAILABILITY STATEMENT

Data available on request from the authors.

ORCID

Carl-Christoph Höhne https://orcid.org/0000-0003-1582-1656

REFERENCES

[1] L. Bravo Diaz, X. He, Z. Hu, F. Restuccia, M. Marinescu, J. V. Barreras, Y. Patel, G. Offer, G. Rein, *J. Electrochem. Soc.* **2020**, *167*, 90559.

[2] United Nations Economic Commission for Europe, Regulation No 100 of the Economic Commission for Europe of the United Nations (UNECE) - Uniform provisions concerning the approval of vehicles with regard to specific requirements for the electric power train, **2015**. https://op.europa.eu/en/publication-detail/-/publication/fd8e6b47-d767-11e4-9de8-01aa75ed71a1.

[3] N. Loypetch, J. Tröltzsch, D. Nestler, L. Kroll, S. Siengchin, *Struct. Mater.* **2021**, *23*, 301.

[4] J. Grünewald, P. Parlevliet, V. Altstädt, *J. Thermoplast. Compos. Mater.* **2017**, *30*, 437.

[5] C. Ageorges, L. Ye, M. Hou, *Compos. Part A: Appl. Sci. Manuf.* **2001**, *32*, 839.

[6] M. Akermo, B. T. Astrom, *J. Thermoplast. Compos. Mater.* **1999**, *12*, 297.

[7] O. Skawinski, C. Binetruy, P. Krawczak, J. Grando, E. Bonneau, *Struct. Mater.* **2004**, *6*, 399.

[8] C. A. Wilkie, A. B. Morgan Eds., *Fire Retardancy of Polymeric Materials*, 2nd ed., CRC Press, Boca Raton, FL **2010**.

[9] E. D. Weil, S. V. Levchik, *Flame Retardants for Plastics and Textiles: Practical Applications*, 2nd ed., Hanser Publishers, Munich, Cincinnati **2016**.

[10] R. Sauerwein, Mineral filler flame retardants. in *Non-Halogenated Flame Retardant Handbook* (Eds: A. B. Morgan, C. A. Wilkie), John Wiley & Sons, Inc, Hoboken, NJ **2014**, p. 75.

[11] B. Schartel, T. R. Hull, *Fire Mater.* **2007**, *31*, 327.

How to cite this article: C.-C. Höhne, V. Gettwert, S. Kilian, B. Tillner, I. Jahn, A. Menrath, *SPE Polym.* **2022**, 1. https://doi.org/10.1002/pls2.10068